SYNTHESIS OF CURCUMIN-FERULIC ACID CONJUGATE VIA STEGLICH ESTERIFICATION AND ANTI-LUNG CANCER ACTIVITY OF AGAINST HUMAN NON-SMALL LUNG CANCER CELLS (NSLCC)

XI CHENG [1], ZHIGANG ZUO [2], QIHUI ZHOU [3], PING MA [1], XINLI LIU [4]*

[1] *Department of Respiratory, Anhui Zhongke Gengjiu Hospital, Hefei Anhui,230041, China.*
[2] *Department of Cardiothoracic Surgery, Ezhou Central Hospital, Ezhou Hubei, 436000, China.*
[3] *Department of Respiratory and Critical Care Medicine, Anhui Zhongke Gengjiu Hospital, Hefei, Anhui ,230041, China.*
[4] *Department of Nursing, Huanggang Polytechnic College, Huanggang, Hubei, 438002, China.*

ABSTRACT

In the current work, the conjugate of curcumin and ferulic acid (compound 1) was developed and then examined utilizing a battery of biochemical assays to assess its pharmacological effectiveness against lung cancer. The compound 1 was synthesized using steglich esterification in excellent yield and then evaluated for its ability to inhibit the growth of different types of human cancer cells, including cells of the gastric cancer (SGC-7901), breast cancer (MCF7), liver cancer (HepG-2), lung cancer (A549), and human cervical carcinoma (HeLa). It exhibited stronger inhibitory effects on A549 cells compared to the other cell types, indicating its potent anti-lung cancer activity. It induces substantial suppression of many kinases, including EGFR, PI3K, mTOR, and VEGFR2. It exhibited cell cycle suppression of G2/M phase, resulting in a significant rise in apoptosis rate in A549 cells. Compound 1 showed a notable suppression of telomerase activity and a rise in the depolarization of mitochondrial membrane potential in A549 cells. The present study showcased the creation of a curcumin-ferulic acid conjugate (referred to as Compound 1) as a very potent anticancer medication that selectively targets lung cancer cells.

Keywords: Lung cancer, kinase, apoptosis, cell cycle, telomerase activity.

1. INTRODUCTION

Despite the therapeutic and diagnostic advances, cancer remains a worldwide concern for mankind [1]. With an anticipated 2 million new cases and 1.8 million fatalities in 2020, lung cancer ranks first among human malignancies in terms of both incidence and mortality [2]. The biological features and clinical outcomes of small-cell lung cancer (SCLC) and non-small-cell lung cancer (NSCLC) allow for their further categorization. Small cell lung cancer makes up around 15-20% of all lung cancers, in contrast to non-small cell lung cancer, which makes up 80-85% of lung cancers and can be further split into adenocarcinoma, squamous cell carcinoma, and large cell carcinoma [3]. Depending on the stage of the disease, NSCLC was shown to be responsible for around 85 percent of all cases, and the survival rate over five years ranged from 50 to 17 percent. Unless the type of non-small cell lung cancer is sensitive to specific targeted treatments, like kinase inhibitors, the prognosis is not good [4].

The leading cause of cancer-related mortality among Americans, regardless of gender, is lung cancer, which is expected to have 238,340 new cases and 127,070 fatalities in 2023[5]. Lung cancer claims more lives than any other cancer in the body, including prostate, colorectal, breast, and brain cancers put together. Lung cancer death rates have dropped thanks to advancements in tumor biology research, early cancer detection, and precision oncology driven by biomarkers. The global smoking rate has dropped significantly as a result of public education campaigns, which in turn has reduced the incidence of lung cancer[6]. It is a complex disease with a diverse and intricate patient group, making its care difficult. The management is affected by a multitude of parameters, such as stage, histology, age, comorbidities, symptoms, patient performance level, and preference. The gold standard for NSCLS treatment is a platinum-based doublet chemotherapy regimen paired with definitive local therapy, which can be radiation or surgery[7]. Some individuals with stage IIIA illness prefer surgery as a treatment option. Mediastinal node disease burden, performance level, and medical comorbidities inform the choice of local therapy modality (radiation vs. surgery). Patients with fully resected NSCLC can see an improvement of 4-15% in 5-year overall survival with adjuvant chemotherapy[8].

Over the last few decades, we have witnessed that medications used in contemporary medicine, particularly those used to treat cancer, have either originated from plants or may be produced as derivatives of active constituents [9,10]. These active constituents include flavonoids, terpenes, alkaloids, lignans, and other similar compounds. These chemicals exhibited powerful anticancer properties as a result of their antioxidant, anti-inflammatory, and DNA repair, stimulation of apoptosis, immunological stimulation, suppression of the advancement of cell cycles, and interference with embryonic growth processes (including the Notch, Wnt, and Hedgehog pathways) [11,12].

The polyphenol curcumin, obtained from the root of the *Curcuma longa* plant, has several health benefits, and research has demonstrated that it targets various signaling molecules and has a cellular activity to back it up [13]. Several medical ailments, including pain [14], metabolic syndrome [15], inflammation [16], and neuro-degenerative disease [17], have demonstrated improvement after using it. Additionally, it has shown beneficial effects on the kidneys and liver. Acute myeloid leukemia was not the only type of cancer it effectively treated; it also fought against brain, bladder, colon, breast, and prostate cancers [18,19]. It exhibited notable anticancer effects in non-small cell lung cancer as well[20]. Research indicates that its anti-inflammatory and antioxidant properties influence these pharmacological benefits [21].

Ferulic acid (FA), or 4-hydroxy-3-methoxycinnamic acid, is a phenolic compound found in the majority of plants[22]. Studies showed that it exhibits excellent anti-inflammatory and antioxidant properties, and can be used against a range of ailments including diabetes, cancer, lung disease, and cardiovascular disorders [23,24]. It also showed antibacterial, anti-fungal, anti-viral, and hepato-protective activity[25–28].

Ohashi recently shown that combined treatment with curcumin and ferulic acid was more effective than treatment with either compound alone in preventing Aβ-induced neurotoxicity [29]. In addition, Paciello et al. demonstrated that curcumin and ferulic acid have a dual function in the process of combating chemoresistance and cisplatin-induced ototoxicity [30]. Nevertheless, none of the research have recorded the pharmacological impact of the combined structure of curcumin and ferulic acid. This hybrid skeleton is specifically engineered to engage with many targets simultaneously, hence minimizing the chances of drug-drug interactions. Moreover, it exhibits diminished side effects and a decreased tendency to provoke resistance compared to the standalone drug. These unique hybrid compounds are anticipated to possess better affinity, increased efficacy, and improved safety. Thus, in the present study, we intend to determine the bioactivity of curcumin-ferulic acid hybrid conjugate against the NSCLC and its mechanism of action.

2. RESULTS AND DISCUSSION

Synthesis

The synthesis of the title compounds, ferulic acid coupled with curcumin, was accomplished as described in Scheme 1 as per the previously reported procedure [31]. The synthesis of ferulic acid curcumin conjugate (1) was the first step in Scheme 1. This was accomplished by reacting curcumin with ferulic acid at a temperature of 85 degrees Celsius in 1,2-dichloroethane over a period of twenty-four hours. Additionally, N,N'-Dicyclohexylcarbodiimide (DCC) and 4-Dimethylaminopyridine (DMAP) were present. The yield was satisfactory. The esterification process was carried out with DCC serving as the coupling reagent and DMAP serving as the catalyst in this reaction, which is a typical example of Steglich esterification.

**Corresponding author email: lily20220506@sina.com*

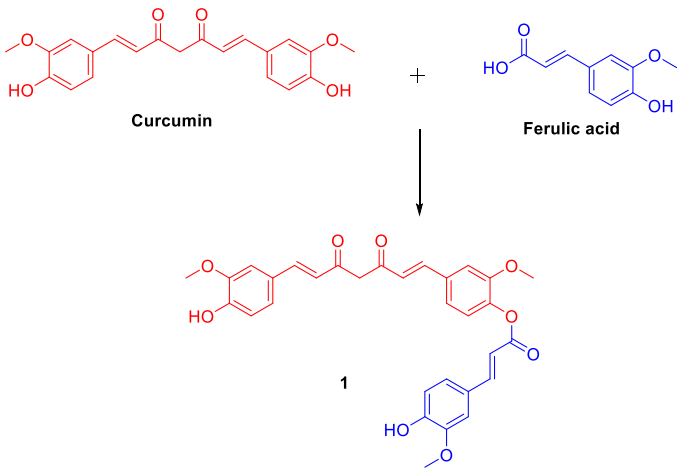

Scheme 1: Synthesis of curcumin-ferulic acid hybrid conjugate (**1**). Reagents and conditions: DCC/DMAP; DCE, 85 °C, 24 h.

Numerous analyses, including FT-IR, ^{1}H NMR, ^{13}C NMR, mass spectrometry, and elemental analysis, validated the structure of compound 1. In addition, the characteristic C-H bands of the phenyl ring were shown at 2918.35 cm^{-1} in the FT-IR spectra. The OCH_3 stretching, prominent bands appeared at 2849.71 cm^{-1}. A prominent band at 1716.83 cm^{-1} is associated with the C=O group. The C-H bond associated with the phenyl ring showed bending vibrations at 1625.48 cm^{-1}. The stretching vibration at 1592.61 cm^{-1}, corresponds to C=C group attached to the phenyl ring. The presence of strong bands at 1162.14 cm^{-1} is due to C-O stretching. Furthermore, the title derivatives were determined using ^{1}H NMR spectra, which indicated doublet peaks at 7.75-6.76 ppm caused by aromatic ring proton. Furthermore, the aliphatic CH proton group in the side chain resulted in doublet peaks at 5.74 ppm. Furthermore, singlet peaks of aliphatic OCH_3 groups associated with phenyl ring proton were observed at 3.87 and 3.84 ppm. The resonance peaks of the title compounds were determined to be 149.1–111.9 ppm due to carbon atoms in curcumin's phenyl ring. The aromatic carbon atoms of the ferulic acid phenyl ring appeared between 149.1 and 111.8 ppm. At 51.9 ppm, the aliphatic carbon atoms of the side chain connection to the phenyl ring showed. At 198.9 ppm, the carbonyl's side chain carbon atoms appeared. Finally, the title compounds were identified using mass and elemental analysis.

Anticancer activity

As shown in Table 1, the anticancer effect of compound **1** was determined on the panel of human cancer cells, such as SGC-7901, MCF7, HepG-2, A549, and Hela cells. The least activity was reported against the SGC-7901 cells, while against MCF7, it showed marginally improved activity. Moderate activity was revealed against the HepG-2 and Hela cells. The most potent inhibitory activity was reported in A549 cells with an IC_{50} of 1.25 µM. The results of the activity suggest that compound 1 showed a pattern of inhibition as follows: A549>HepG2>HeLa>MCF7>SGC7901, revealing potent anti-lung cancer activity. However, the curcumin and ferulic acid in the alone treated group does not exhibit potent activity than the compound 1 against all the tested cell line. No effect on non-cancerous (MCF-12A) cell viability was observed at the highest dose of >200 µM when compound 1, curcumin, and ferulic acid were examined.

Table 1: Anticancer activity of compound 1, curcumin and ferulic acid against human cancer cell lines.

Compound	IC_{50} (in µM)[a]					
	SGC7901	MCF7	HepG2	A549	HeLa	MCF-12A
1	23.45 ± 1.52	18.37 ± 1.44	8.38 ± 1.03	1.25 ± 0.22	12.34 ± 1.26	>200 µM
Curcumin	34.60 ± 2.35	29.04 ± 1.34	38.41 ± 2.93	4.56 ± 0.32	29.72 ± 2.42	>200 µM
Ferulic Acid	54.43 ± 3.24	34.22 ± 3.15	45.15 ± 3.44	9.15 ± 0.65	41.32 ± 2.35	>200 µM
Standard (Cisplatin)	1.25 ± 0.41	2.34 ± 0.33	4.62 ± 0.83	3.63 ± 0.76	4.32 ± 0.85	Not determined

[a] is mean ± SEM

Various studies reported the anticancer activity of curcumin with numerous natural products. Zhang et al. showed the synthesis of a curcumin-piperlongumine (CP) hybrid compound [32]. The conjugate caused cell cycle arrest in the G2/M phase and apoptosis, and it significantly inhibited cell growth. It has been also found that suggests that cell cycle arrest played a role in the apoptosis produced by CP. Also, by manipulating JNK signaling, they proved that CP triggers cell cycle arrest and death. The creation of hybrids with curcumin and resveratrol was shown by Hernández et al., where these hybrid compounds showed significant cytotoxic effect against colorectal cancer cells [33]. Serafim et al. demonstrated that anticancer activity of ferulic acid was potentiated by hybridizing with caffeic against MCF-7 cells [34]. The compound exhibited substantial suppression of cell growth and caused changes in the cell cycle and cell death, particularly affecting MCF-7 cells,

These results were found in accordance with our study, where anticancer activity of curcumin-ferulic acid conjugate was found more potent than curcumin and ferulic acid alone against the lung cancer.

Kinase inhibitory activity

EGFR-TK inhibitory activity

Therapeutic strategies that target epidermal growth factor receptor tyrosine kinase, or EGFR-TKIs, are crucial for patients with EGFR-sensitizing mutations, such as the Ex19del or L858R mutations [35,36]. Patients with NSCLC who carry an EGFR mutation are now entering a new era of treatment with the introduction and widespread use of EGFR-TKIs [37]. This paradigm change has been underlined by significant gains in patient survival and clinical outcomes. Consequently, EGFR-TKIs have emerged as the most effective and widely accepted treatment for NSCLC, particularly as the initial therapy for patients with EGFR mutations. Therefore, in this investigation, we have established the suppressive impact of compound 1 on the EGFR, Table 2

Table 2: Kinase inhibitory effect of compound **1** against various kinases and MMPs

Compound	IC_{50} (in µM)[a]			
	EGFR	PI3K	mTOR	VEGFR2
1	0.78 ± 0.04	2.1 ± 0.05	5.2 ± 0.7	1.3 ± 0.03
Erlotinib	0.003 ± 0.001	-	-	-
Gedatolisib	-	0.021 ± 0.001	0.034 ± 0.002	-
Sorafenib	-	-	-	0.071 ± 0.002

[a] is mean ± SEM

PI3K/mTOR inhibitory activity

PI3K-AKT-mTOR pathway alterations are related with NSCLC [38]. This pathway controls numerous cellular activities, such as adhesion, migration, invasion, survival, and differentiation. Even while EGFR TKIs produce a remarkable clinical response, research shows that resistance will always develop in treated patients due to activation of the PI3K-AKT-mTOR pathway [39]. Patients with EGFR mutations and PI3K pathway activation had a shorter progression-free survival (PFS) and inferior overall survival (OS) in clinical trials [40]. It is particularly advantageous to target PI3K/mTOR in the fight against NSCLC. The results suggest that compound 1 showed significant inhibition of PI3K and mTOR with IC_{50} of 2.1 µM, and 5.2 µM, respectively, Table 2.

VEGFR2 inhibitory activity

The VEFG pathway plays a crucial role in angiogenesis, which contributes to the growth of malignancies, particularly non-small cell lung cancers (NSCLCs) [41]. The VEFG and VEFG receptors have been the focus of numerous newly-approved therapeutic medications for non-small cell lung cancers [42]. The VEFG and EGFR pathways can work independently of each other during oncogenesis, and preclinical research has shown that they share a similar downstream signaling sequence [43]. An increase in VEFG occurs in NSCLCs with an EGFR mutation through hypoxia-independent mechanisms due to the up-regulation of EGFR signaling. Resistance to EGFR tyrosine kinase inhibitors, a form of treatment, develops in part because of this elevated VEFG. Clinical trials demonstrated that EGFR TKIs, when combined with anti-VEFG therapy, considerably improved clinical outcomes. The current investigation has so established that chemical 1 inhibits VEGFR2 activity. Table 2 shows that compound 1 inhibited VEGFR2 activity effectively, with an IC_{50} of 1.3 ± 0.03 µM.

Quantitative Telomerase detection

An essential function of telomeres, which are complexes of nucleoproteins, is to protect the ends of chromosomes. As a result of DNA replication failing during each cell cycle, telomeres shorten[44]. Critical telomere shortening is an important factor in genomic instability, which in turn promotes cancer. The cancer cell uses telomerase, a specialized ribonucleoprotein that regenerates telomeric DNA, to keep its shortened telomeres. This procedure allows tumors to thrive and grow unchecked. Consequently, a new approach including Telomerase has been proposed as a way to combat chemotherapy resistance and NSCLC-targeted treatment [45]. We measured compound 1's impact on telomerase activity in A549 cells in this work. The results of the comparison between compound 1 and the standard BIBR 1532 are reported in Table 3. Compound 1 inhibited telomerase activity at a higher rate in comparison to BIBR 1532 (62.4% vs. 52.3%).

Table 3: Telomerase activity assay of compound 1.

Compound	% Inhibition
Compound 1	62.4
BIBR1532	52.3
Control	0

Rate of Apoptosis and cell cycle analysis

Recognizing the interconnectedness of apoptosis and cell cycle progression in cancer cell survival and proliferation, anticancer medicines frequently aim to target these processes [46]. Through activating pro-apoptotic pathways or suppressing anti-apoptotic signals, a number of medications can cause apoptosis, which ultimately results in the elimination of cancer cells. Also, some medications can stop cancer cells from dividing and multiplying by inducing cell cycle arrest [47]. Because cells at the cell cycle halt may go through apoptosis if the damage is too great to be repaired, the interaction between DNA damage and apoptosis is vital in cancer treatment. A thorough understanding of the complex relationship between cell cycle progression and apoptosis, as well as the ability to control this balance, is necessary for the effective creation of anticancer drugs that selectively target cancer cells without harming healthy tissues [48]. As can be shown in Figure 1a of the current work, compound 1 significantly and concentration-dependently increases the rate of apoptosis in A549 cells. There was a decrease in the S-phase cell population and an increase in the number of cells in G2/GM phase in the treated group. The G0/G1 phase did not undergo any changes. Compound 1's ability to cause apoptosis and hamper cell cycle progression, particularly at the G2/M stage, is thus proposed as the mechanism by which it inhibits the proliferation of A549 cells, Fig. 1b.

Mitochondrial membrane potential

The mitochondrial membrane potential plays a crucial role in determining the effectiveness of several cancer medications. This metric is useful for measuring the electrochemical gradient across the inner mitochondrial membrane, which is essential for ATP production and cell survival [49]. The impairment of mitochondrial membrane potential can result in impaired mitochondrial function, the secretion of pro-apoptotic elements, and the initiation of apoptosis. Several chemotherapeutic agents, including cisplatin and doxorubicin, specifically act on MMP, causing its degradation and subsequent apoptosis[50]. These medications have the ability to trigger apoptosis specifically in malignant tissues by selectively targeting cancer cells, which frequently have elevated levels of MMP in comparison to normal cells [51]. Hence, comprehending and controlling MMP holds great potential as a technique for creating innovative anticancer treatments that exhibit enhanced effectiveness and specificity. Prior to flow cytometry analysis, the A549 treated cells were collected and stained with JC-1. Figure 2 shows the results of a 24-hour study estimating compound 1's influence on MMP in A549 cells. The study used JC-1 disaggregation, which correlates with mitochondrial membrane potential loss, at the stated doses. Compound 1 significantly increases Δψm (% depolarized) compared to non-treated cells, according to the data. So, it has been postulated that compound 1 causes A549 cells to undergo apoptosis via depolarizing the potential of the mitochondrial membrane.

Our investigation has various limitations, including the need to generate additional curcumin derivatives in order to obtain more SAR data for the development of the lead chemical. Additionally, it would be prudent to investigate the pharmacokinetic investigations of chemical 1.

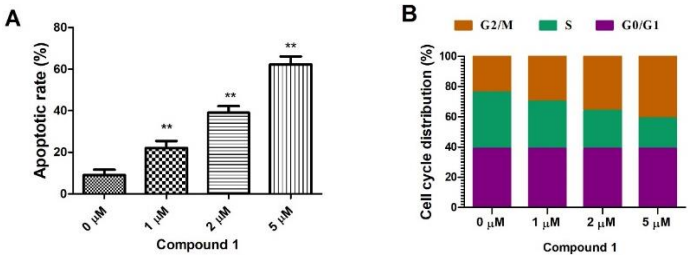

Figure 1. Effect of compound 1 on the a) apoptotic rate and b) cell cycle distribution of A549 cells. Data presented as mean ± SEM (n = 3). ** $p<0.05$ *vs.* non-treated group.

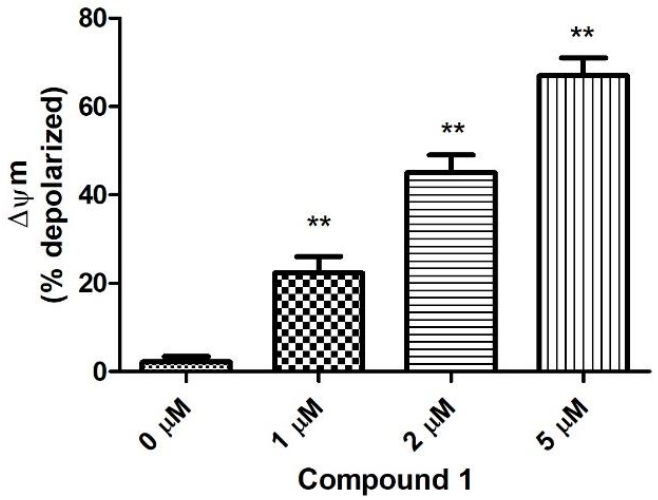

Figure 2. Effect of compound 1 on mitochondrial membrane potential (Δψm) of A549 cells. Data presented as mean ± SEM (n = 3). ** $p<0.05$ *vs.* non-treated group.

CONCLUSION

The current investigation demonstrated the synthesis of curcumin-ferulic acid combination (compound 1) as a very effective anticancer drug specifically targeting lung cancer cells, surpassing its efficacy against other types of cancer cells. The results demonstrated a notable suppression of many kinases, including EGFR, PI3K, mTOR, and VEGFR2. The suppression of the cell cycle in the G2/M phase resulted in a considerable increase in the rate of apoptosis in compound 1 treated A549 cells. A notable suppression of telomerase activity and an elevation in the depolarization of mitochondrial membrane potential in a concentration-dependent manner was observed in A549 cells treated with compound 1.

EXPERIMENTAL

Chemistry

Sigma Aldrich (USA) supplied the compounds, and they were utilized without additional purification. E. Merck's (0.20 mm) silica gel 60 F254 plates were used for thin-layer chromatography (TLC) experiments (Darmstadt, Germany). A Bruker IFS 66v/S Fourier-transform infrared spectroscopy (FT-IR) instrument was used to record infrared spectra in KBr pellets. A Bruker Avance-400, 100 NMR spectrometer was used to record ^{1}H NMR spectra and ^{13}C NMR spectra in DMSO-d6. The internal reference for these spectrometers was TMS. The results of the elemental analysis, which were done using the Vario elemental analyzer, were within ± 0.4% of the theoretical values and agreed with the suggested structures. A Waters ZQ LC/MS (Liquid chromatography/mass spectrometry) single quadrupole system with an electrospray ionization (ESI) source was used to record the low-resolution mass spectra (MS).

Synthesis

The synthesis was performed as per the previously reported procedure [31]. Briefly the solution of 1,2-dichloroethane, curcumin (0.001 mol) and trans-ferulic acid (0.001 mol) were mixed and stirred. In the equal amount (0.05 mol) N, N'-Dicyclohexylcarbodiimide (DCC) and 4-methylaminopyridine (DMAP) were introduced to the above mixture. The reaction mixture was filtered after being stirred at 85°C for 24 hours, and the filtrate was then washed with distilled water. The mixed organic layers were extracted with dichloromethane (DCM) twice, washed with brine, and then dried over Na2SO4. Under reduced pressure, the solvent (dichloromethane) was evaporated. In order to obtain compound 1, the raw material was subjected to chromatography using silica gel through dichloromethane (DCM).

4-((1E,6E)-7-(4-hydroxy-3-methoxyphenyl)-3,5-dioxohepta-1,6-dien-1-yl)-2-methoxyphenyl (E)-3-(4-hydroxy-3-methoxyphenyl)acrylate

Yield: 76 %; MW: 544.56 ; R_f: 0.64; FTIR (ν_{max}; cm^{-1} KBr): 3503.82 (O-H stretching), 2918.35 (Aromatic C-H stretching), 2849.71 (OCH_3 stretching), 1716.83 (C=O stretching), 1625.48 (C-H bending), 1592.61 (C=C stretching), 1162.14 (C-O stretching), ; ^{1}H NMR (400MHz, $DMSO^{-d6}$, TMS) δ ppm: 9.57 (s, 2H, 2×O-H), 7.79 (d, 1 H, *J*=15.69Hz, CH), 7.75 (d, 1H, *J*=1.97 Hz, Ar-H), 7.69 (d, 1H, J=1.93 Hz, Ar-H), 7.64 (d, 1H, *J*=1.94 Hz, Ar-H), 7.45 (d, 1H, *J*=0.55Hz, Ar-H), 7.26 (d, 1H, *J*=0.47Hz, Ar-H), 7.25 (d, 1H, *J*=0.42Hz, Ar-H),7.23 (d, 1H, *J*=0.47 Hz, Ar-H), 6.78 (d, 1H, *J*=0.41 Hz, Ar-H), 6.76 (d, 1H, *J*=0.42 Hz, Ar-H), δ=3.84 (s, 3 H, OCH_3), 3.87 (s, 6 H OCH_3), 5.94 (s, 2 H, CH_2), 5.74 (d, 1H, *J*=9.4Hz, CH), 7.43 (d, 1H, *J*=9.2 Hz, CH), 6.82 (d, 1H, *J*=15.62 Hz, CH), 6.71 (d, 1H, *J*=15.69 Hz, CH), 7.72 (d, 1H, *J*=15.67Hz, CH); ^{13}C NMR (100MHz, $DMSO^{-d6}$) δ ppm: 198.9, 164.3, 149.1,147.9, 142.8, 131.8, 130.4, 127.6, 122.9, 115.5, 116.8, 111.9, 110.9, 56.1, 55.8 51.9; Mass: 545.58 (M+H)+; Elemental analysis for $C_{31}H_{28}O_9$: Calculated: C, 68.38; H, 5.18;.Found: C, 68.41; H, 5.17.

Cells

Human gastric cancer cell line (SGC-7901), breast cancer cell line (MCF7), liver cancer cell line (HepG-2), lung cancer cell line (A549), and human cervical carcinoma cell line (HeLa) were obtained from the American Type Culture Collection (ATCC, USA) and cultured as per the instructed protocol.

MTT cytotoxicity assay

To evaluate chemical 1's impact on cancer cell growth, a previously described approach known as the MTT [3-(4,5-dimethylthiazol-2-yl)-2,5-diphenyltetrazoliumbromide] assay was employed [52]. Before being treated with compound 1, the cells were cultivated on 96-well flat-bottom microtiter culture plates at a density of 5x104 cells per well. Afterwards, 20 µL of fresh MTT solution (2.5 mg/ml) was added to the cells and left to treat them at 37°C for 4 hours. To dissolve the formazan, DMSO was then added. Lastly, a microplate reader was used to measure the absorbance at 570 nm.

Kinase inhibitory activity

The kinase inhibitory activity was determined as per the manufacturer's instructions and the details of the kits are as follows a) EGFR kinase inhibitory activity: EGFR (epidermal growth factor receptor) Kinase Assay Kit, Abcam, Cambridge, MA, USA; VEGFR2 (vascular endothelial growth factor receptor 2) kinase inhibitory activity: VEGFR2 Kinase Assay Kit, BPS Biosciences, San Diego, CA, USA); c) PI3K (phosphoinositide 3-kinases) kinase inhibitory activity: PI3Kβ (p110β/p85α) assay kit (BPS Bioscience, San Diego, CA, USA), using ADP-Glo® Kinase Assay; mTOR (mammalian target of rapamycin) kinase inhibitory activity: K-LISA™ mTOR Activity Kit (Merck-Calbiochem, Germany).

Quantitative Telomerase detection

Using a quantitative telomerase detection kit (QTD kit, US Biomax, U.S.A.), the telomerase activity was evaluated. In brief, 1 × lysis buffer was used to lyse the cells, and they were left to react at 4°C for 30 minutes. After that, the lysate was spun at 12,000 × g for 20 minutes at 4°C, which allowed the supernatant to be collected. A Bio-Rad protein assay was used to determine the quantity of proteins in the cell lysate. In order to conduct real-time amplifications, the ABI Prism 7300 Sequence Detection System (Applied Biosystems, CA, U.S.) was utilized. A comparative threshold cycle (Ct) was used to measure telomerase activity. This Ct has an inverse correlation with the Ct of real-time PCR [53].

Annexin V/propidium iodide (PI) staining assay

After being treated with compound 1 at different concentrations (1, 2, and 5 µM), the cells were washed three times with cold PBS and then resuspended in binding buffer. The cells were left to incubate in the dark for 10 minutes after being treated with FITC-annexin V at a final concentration of 1 mg/L. Next, the cells were washed with PBS once again, spun in a centrifuge, and finally redissolved in 100 µL of binding buffer. Following 5 minutes of incubation, the cells were promptly examined using a flow cytometer (Becton Dickinson, Rahway, New Jersey, USA) after being exposed to a final concentration of 2 mg/L of PI [54].

Cell cycle analysis

We assessed cell proliferation using propidium iodide (PI) staining. The process began with the seeding of cells in 6-well plates with medium at a density of 1×106 cells/well, followed by overnight incubation. After being rinsed with PBS, the cells were subjected to 72 hours of treatment with compound 1 at doses of 1, 2, and 5 µM in a medium. After the cells were fixed with 70% ethanol for 18 hours at 4°C, they were stained with 500 µL of PI solution including RNase in the dark for 20 minutes at room temperature. Furthermore, the cells were analyzed using flow cytometry, using a BD Accuri C6 flow cytometer from BD Biosciences [55,56].

Mitochondrial membrane potential

The cells (at 1×10^5 cells/well) were cultured in a 6-well plate at a density of 5×10^5 cells per well. The plates were then incubated at 37°C overnight. The RPMI-1640 medium was removed and the cells were cultured in a fresh RPMI-1640 medium containing compound 1 at varying doses (0, 1, 2 and 5 µM) for 24 hrs or 24 of incubation. Afterwards, the cells were collected and incubated with JC-1 (10 µg/ml) reagent and MitoSOX Red (Molecular Probes Inc., Eugene, OR, USA) at 37°C for 30 min for detection of the mitochondrial membrane potential as per the manufacturer's instruction.

STATISTICAL ANALYSIS

The values were reported as the mean ± standard error of mean (SEM). The One-Way ANOVA analysis of variance and the posthoc Duncan test were employed in GraphPad Prism v.8, USA to identify the disparities in the means of the groups. $P < 0.05$ was found to be the level of statistical significance for the results [57]

ACKNOWLEDGEMENTS

None

DECLARATION OF CONFLICTING INTERESTS

The authors declared no potential conflicts of interest with respect to the research, authorship, and/or publication of this article.

ETHICAL APPROVAL

There are no animal or human in this article and ethical approval is not applicable.

FUNDING

The study has been funded by Ezhou City science and technology plan project（EZ01-002-20210137).

STATEMENT OF INFORMED CONSENT

There are no human subjects in this article and informed consent is not applicable.

REFERENCES

1. Latimer KM, Mott TF. Lung cancer: Diagnosis, treatment principles, and screening. Am Fam Physician 2015. https://doi.org/d11787 [pii].
2. Sung H, Ferlay J, Siegel RL, Laversanne M, Soerjomataram I, Jemal A, et al. Global Cancer Statistics 2020: GLOBOCAN Estimates of Incidence and Mortality Worldwide for 36 Cancers in 185 Countries. CA Cancer J Clin 2021;71:209–49. https://doi.org/10.3322/caac.21660.
3. Bray F, Ferlay J, Soerjomataram I, Siegel RL, Torre LA, Jemal A. Global cancer statistics 2018: GLOBOCAN estimates of incidence and mortality worldwide for 36 cancers in 185 countries. CA Cancer J Clin 2018;68:394–424. https://doi.org/10.3322/caac.21492.
4. Xiao Y, Liu P, Wei J, Zhang X, Guo J, Lin Y. Recent progress in targeted therapy for non-small cell lung cancer. Front Pharmacol 2023;14. https://doi.org/10.3389/fphar.2023.1125547.
5. Wolf AMD, Oeffinger KC, Shih TY, Walter LC, Church TR, Fontham ETH, et al. Screening for lung cancer: 2023 guideline update from the American Cancer Society. CA Cancer J Clin 2024;74. https://doi.org/10.3322/caac.21811.
6. Kratzer TB, Bandi P, Freedman ND, Smith RA, Travis WD, Jemal A, et al. Lung cancer statistics, 2023. Cancer 2024;130. https://doi.org/10.1002/cncr.35128.
7. Raskova Kafkova L, Mierzwicka JM, Chakraborty P, Jakubec P, Fischer O, Skarda J, et al. NSCLC: from tumorigenesis, immune checkpoint misuse to current and future targeted therapy. Front Immunol 2024;15. https://doi.org/10.3389/fimmu.2024.1342086.
8. Lim JU. Update on Adjuvant Treatment in Resectable Non-Small Cell Lung Cancer and Potential Biomarkers Predicting Postoperative Relapse. Tuberc Respir Dis (Seoul) 2023;86. https://doi.org/10.4046/trd.2022.0081.
9. Butler MS. Natural products to drugs: Natural product-derived compounds in clinical trials. Nat Prod Rep 2008;25:475–516. https://doi.org/10.1039/b514294f.
10. Mang CP, Haustedt LO. Natural product scaffolds in cancer therapy. Natural Products and Cancer Drug Discovery, 2013, p. 123–73. https://doi.org/10.1007/978-1-4614-4654-5_6.
11. Rayan A, Raiyn J, Falah M. Nature is the best source of anticancer drugs: Indexing natural products for their anticancer bioactivity. PLoS One 2017;12. https://doi.org/10.1371/journal.pone.0187925.
12. Naeem A, Hu P, Yang M, Zhang J, Liu Y, Zhu W, et al. Natural Products as Anticancer Agents: Current Status and Future Perspectives. Molecules 2022;27. https://doi.org/10.3390/molecules27238367.
13. Hewlings SJ, Kalman DS. Curcumin: A review of its effects on human health. Foods 2017;6. https://doi.org/10.3390/foods6100092.
14. Sun J, Chen F, Braun C, Zhou YQ, Rittner H, Tian YK, et al. Role of curcumin in the management of pathological pain. Phytomedicine 2018;48. https://doi.org/10.1016/j.phymed.2018.04.045.
15. Pivari F, Mingione A, Brasacchio C, Soldati L. Curcumin and type 2 diabetes mellitus: Prevention and treatment. Nutrients 2019;11. https://doi.org/10.3390/nu11081837.
16. Garodia P, Hegde M, Kunnumakkara AB, Aggarwal BB. Curcumin, inflammation, and neurological disorders: How are they linked? Integr Med Res 2023;12. https://doi.org/10.1016/j.imr.2023.100968.
17. Ghosh S, Banerjee S, Sil PC. The beneficial role of curcumin on inflammation, diabetes and neurodegenerative disease: A recent update. Food and Chemical Toxicology 2015;83. https://doi.org/10.1016/j.fct.2015.05.022.
18. Giordano A, Tommonaro G. Curcumin and cancer. Nutrients 2019;11. https://doi.org/10.3390/nu11102376.
19. Zoi V, Galani V, Lianos GD, Voulgaris S, Kyritsis AP, Alexiou GA. The role of curcumin in cancer treatment. Biomedicines 2021;9. https://doi.org/10.3390/biomedicines9091086.
20. Tang X, Ding H, Liang M, Chen X, Yan Y, Wan N, et al. Curcumin induces ferroptosis in non-small-cell lung cancer via activating autophagy. Thorac Cancer 2021;12. https://doi.org/10.1111/1759-7714.13904.
21. He Y, Yue Y, Zheng X, Zhang K, Chen S, Du Z. Curcumin, inflammation, and chronic diseases: How are they linked? Molecules 2015;20. https://doi.org/10.3390/molecules20059183.
22. Li D, Rui Y xin, Guo S duo, Luan F, Liu R, Zeng N. Ferulic acid: A review of its pharmacology, pharmacokinetics and derivatives. Life Sci 2021;284. https://doi.org/10.1016/j.lfs.2021.119921.
23. de Paiva LB, Goldbeck R, dos Santos WD, Squina FM. Ferulic acid and derivatives: Molecules with potential application in the pharmaceutical field. Brazilian Journal of Pharmaceutical Sciences 2013;49. https://doi.org/10.1590/S1984-82502013000300002.
24. Marcato DC, Spagnol CM, Salgado HRN, Isaac VLB, Corrêa MA. New and potential properties, characteristics, and analytical methods of ferulic acid: A review. Brazilian Journal of Pharmaceutical Sciences 2022;58. https://doi.org/10.1590/s2175-97902020000118747.
25. Li X, Wu J, Xu F, Chu C, Li X, Shi X, et al. Use of Ferulic Acid in the Management of Diabetes Mellitus and Its Complications. Molecules 2022;27. https://doi.org/10.3390/molecules27186010.
26. Zhang X, Lin D, Jiang R, Li H, Wan J, Li H. Ferulic acid exerts antitumor activity and inhibits metastasis in breast cancer cells by regulating epithelial to mesenchymal transition. Oncol Rep 2016;36. https://doi.org/10.3892/or.2016.4804.
27. Sin Singer Brugiolo A, Carvalho Gouveia AC, de Souza Alves CC, de Castro e Silva FM, Esteves de Oliveira É, Ferreira AP. Ferulic acid supresses Th2 immune response and prevents remodeling in ovalbumin-induced pulmonary allergy associated with inhibition of epithelial-derived cytokines. Pulm Pharmacol Ther 2017;45. https://doi.org/10.1016/j.pupt.2017.07.001.
28. Neto-Neves EM, da Silva Maia Bezerra Filho C, Dejani NN, de Sousa DP. Ferulic Acid and Cardiovascular Health: Therapeutic and Preventive Potential. Mini-Reviews in Medicinal Chemistry 2021;21. https://doi.org/10.2174/1389557521666210105122841.
29. Ohashi H, Tsuji M, Oguchi T, Momma Y, Nohara T, Ito N, et al. Combined Treatment with Curcumin and Ferulic Acid Suppressed the Aβ-Induced Neurotoxicity More than Curcumin and Ferulic Acid Alone. Int J Mol Sci 2022;23. https://doi.org/10.3390/ijms23179685.
30. Paciello F, Rita Fetoni A, Mezzogori D, Rolesi R, Di Pino A, Paludetti G, et al. The dual role of curcumin and ferulic acid in counteracting chemoresistance and cisplatin-induced ototoxicity. Sci Rep 2020;10. https://doi.org/10.1038/s41598-020-57965-0.
31. Law S, Lo C, Han J, Yang F, Leung AW, Xu C. Design, Synthesis and Characterization of Novel Curcumin Derivatives. Nat Prod Chem Res 2020;8. https://doi.org/10.35248/2329-6836.20.8.367.
32. Zhang Q, Hui M, Chen G, Huang H, Wang S, Ye Y, et al. Curcumin-Piperlongumine Hybrid Molecule Increases Cell Cycle Arrest and Apoptosis in Lung Cancer through JNK/c-Jun Signaling Pathway. J Agric Food Chem 2024;72. https://doi.org/10.1021/acs.jafc.4c00882.
33. Hernández C, Moreno G, Herrera-R A, Cardona-G W. New hybrids based on curcumin and resveratrol: Synthesis, cytotoxicity and antiproliferative activity against colorectal cancer cells. Molecules 2021;26. https://doi.org/10.3390/molecules26092661.
34. Serafim TL, Carvalho FS, Marques MPM, Calheiros R, Silva T, Garrido J, et al. Lipophilic caffeic and ferulic acid derivatives presenting cytotoxicity against human breast cancer cells. Chem Res Toxicol 2011;24. https://doi.org/10.1021/tx200126r.
35. Le X, Nilsson M, Goldman J, Reck M, Nakagawa K, Kato T, et al. Dual EGFR-VEGF Pathway Inhibition: A Promising Strategy for Patients With EGFR-Mutant NSCLC. Journal of Thoracic Oncology 2021;16. https://doi.org/10.1016/j.jtho.2020.10.006.
36. Zhang Z, Stiegler AL, Boggon TJ, Kobayashi S, Halmos B. EGFR-mutated lung cancer: a paradigm of molecular oncology. Oncotarget 2010;1. https://doi.org/10.18632/oncotarget.186.
37. Qiao M, Jiang T, Liu X, Mao S, Zhou F, Li X, et al. Immune Checkpoint Inhibitors in EGFR-Mutated NSCLC: Dusk or Dawn? Journal of Thoracic Oncology 2021;16. https://doi.org/10.1016/j.jtho.2021.04.003.
38. Garcia-Echeverria C, Sellers WR. Drug discovery approaches targeting the PI3K/Akt pathway in cancer. Oncogene 2008;27:5511–26. https://doi.org/10.1038/onc.2008.246.
39. Fumarola C, Bonelli MA, Petronini PG, Alfieri RR. Targeting PI3K/AKT/mTOR pathway in non small cell lung cancer. Biochem Pharmacol 2014. https://doi.org/10.1016/j.bcp.2014.05.011.
40. Jiang L, Zhang J, Xu Y, Xu H, Wang M. Treating non-small cell lung cancer by targeting the PI3K signaling pathway. Chin Med J (Engl) 2022;135. https://doi.org/10.1097/CM9.0000000000002195.
41. Mabeta P, Steenkamp V. The VEGF/VEGFR Axis Revisited: Implications for Cancer Therapy. Int J Mol Sci 2022;23. https://doi.org/10.3390/ijms232415585.
42. Zhao Y, Guo S, Deng J, Shen J, Du F, Wu X, et al. VEGF/VEGFR-Targeted Therapy and Immunotherapy in Non-small Cell Lung Cancer: Targeting the Tumor Microenvironment. Int J Biol Sci 2022;18. https://doi.org/10.7150/ijbs.70958.
43. Wang Q, Zeng A, Zhu M, Song L. Dual inhibition of EGFR VEGF: An effective approach to the treatment of advanced non small cell lung cancer with EGFR mutation (Review). Int J Oncol 2023;62. https://doi.org/10.3892/ijo.2023.5474.
44. Lansdorp PM. Telomeres, Telomerase and Cancer. Arch Med Res 2022;53. https://doi.org/10.1016/j.arcmed.2022.10.004.

45. Tian X, Chen B, Liu X. Telomere and telomerase as targets for cancer therapy. Appl Biochem Biotechnol 2010;160. https://doi.org/10.1007/s12010-009-8633-9.
46. Elmore S. Apoptosis: A Review of Programmed Cell Death. Toxicol Pathol 2007;35:495–516. https://doi.org/10.1080/01926230701320337.
47. Lowe SW, Lin AW. Apoptosis in cancer. Carcinogenesis 2000;21:485–95. https://doi.org/10.1093/carcin/21.3.485.
48. Evan GI, Vousden KH. Proliferation, cell cycle and apoptosis in cancer. Nature 2001. https://doi.org/10.1038/35077213.
49. Ly JD, Grubb DR, Lawen A. The mitochondrial membrane potential (δψm) in apoptosis; an update. Apoptosis 2003;8:115–28. https://doi.org/10.1023/A:1022945107762.
50. Lopez J, Tait SWG. Mitochondrial apoptosis: Killing cancer using the enemy within. Br J Cancer 2015;112. https://doi.org/10.1038/bjc.2015.85.
51. Liu Y, Lu S, Wu L lei, Yang L, Yang L, Wang J. The diversified role of mitochondria in ferroptosis in cancer. Cell Death Dis 2023;14. https://doi.org/10.1038/s41419-023-06045-y.
52. Srivastava JK, Pillai GG, Bhat HR, Verma A, Singh UP. Design and discovery of novel monastrol-1,3,5-triazines as potent anti-breast cancer agent via attenuating Epidermal Growth Factor Receptor tyrosine kinase. Sci Rep 2017;7:5851. https://doi.org/10.1038/s41598-017-05934-5.
53. Darekar SD, Mushtaq M, Gurrapu S, Kovalevska L, Drummond C, Petruchek M, et al. Mitochondrial ribosomal protein S18-2 evokes chromosomal instability and transforms primary rat skin fibroblasts. Oncotarget 2015;6. https://doi.org/10.18632/oncotarget.4123.
54. Wang Z, Zuo J, Zhang L, Zhang Z, Wei Y. Plantamajoside promotes metformin-induced apoptosis, autophagy and proliferation arrest of liver cancer cells via suppressing Akt/GSK3β signaling. Hum Exp Toxicol 2022;41. https://doi.org/10.1177/09603271221078868.
55. Hao M, Zhang K, Wang H, Wang J, Li J, Cheng R, et al. Paeonol Inhibits Glioma Growth In Vivo and In Vitro by Inducing Apoptosis and Cell Cycle Arrest. Revista Brasileira de Farmacognosia 2023;33. https://doi.org/10.1007/s43450-023-00380-z.
56. Du J, Zhao Y, Hu D, Li H, Gao L, Xing X, et al. Pinosylvin Inhibits Esophageal Squamous Cell Carcinoma Migration and Invasion by Regulating STX6/ITGA3/VASP Pathway. Revista Brasileira de Farmacognosia 2023;33. https://doi.org/10.1007/s43450-022-00354-7.
57. Ning Y, Fu Y ling, Zhang QH, Zhang C, Chen Y. Inhibition of in vitro and in vivo ovarian cancer cell growth by pinoresinol occurs by way of inducing autophagy, inhibition of cell invasion, loss of mitochondrial membrane potential and inhibition Ras/MEK/ERK signalling pathway. Journal of BUON 2019;24.